Asian Journal of Chemistry; Vol. 24, No. 7 (2012), 3028-3032

ASIAN JOURNAL OF CHEMISTRY

www.asianjournalofchemistry.co.in

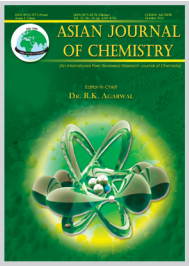

Electrochemical Studies of Tin in the non-Cl^- [EMIm]BF_4 Room Temperature Ionic Liquid

HUI CANG*, WENYAN SHI, JINGLING SHAO and QI XU

Chemical and Biological Engineering College, Yancheng Institute of Technology, Yancheng 224051, Jiangsu, P.R. China

*Corresponding author: Fax: +86 515 88298618; Tel: +86 515 88298611; E-mail: canghui@ycit.edu.cn

(*Received*: 2 July 2011; *Accepted*: 10 February 2012) AJC-11059

The electrochemistry of tin at platinum and glass carbon electrode was studied in the non-Cl^- [EMIm]BF_4 ionic liquid at ambient temperature. The formal potential of the Sn(II)/Sn couple in the non-Cl^- [EMIm]BF_4 is -0.64V *vs*. Ag/Ag(I). The results of cyclic voltammograms indicated that the reduction of Sn(II) on Pt electrode was quasi- or irreversible, the standard heterogeneous rate constant was estimated to be 3.61×10^{-4} cm s^{-1}. The Stokes-Einstein product of Sn(II) in the non-Cl^- [EMIm]BF_4 is, 11.8×10^{-10} g cm s^{-2} K^{-1}, larger than that in free-Cl^- [EMIm]BF_4, suggesting that Sn(II) may exists as bare cation in non-Cl^- [EMIm]BF_4 without complexing agents. The electrodeposition of Sn(II) at glass carbon electrode was complicated by nucleation. Experimental current-time transients are in good agreement with the theoretical model based on 3D nucleation. The morphology examined by SEM of the electrodeposit indicates that the Sn deposit is not a continuous plating film on Pt surface.

Key Words: Tin, Electrochemistry, Ionic liquid, Tetrafluoroborate.

INTRODUCTION

Recently, tremendous research efforts have been devoted to water- and air-stable room temperature ionic liquids (RTILs) obtained by substituting the tetrachloroaluminate chloride anion with water-stable anions such as tetrafluoroaluminate (BF_4^-) and hexafluorophosphate(PF_6^-)[1-4]. Similar to the well known chloroaluminate-based ionic liquids, these water-stable ionic liquids exhibit several attractive properties, such as wide electrochemical window, good thermal and chemical stability and high ionic conductivity. In addition, these new ionic liquids do not display reactivity with air and water, which is the major drawback of the chloro-aluminate-based ionic liquids. Consequently, these room temperature ionic liquids are finding a variety of applications in the field of applied electrochemistry, *e.g.*, rechargeable batteries, capacitors, photoelectrochemical cells, fuel cells, nuclear waste treatment, electrocatalysis, electrosynthesis and electroplating[5-8].

Tin and tin alloys are materials widely used to improve corrosion resistance, enhance appearance and increase solderability[9,10]. They are used to produce numerous metal devices in terms of electrodeposition and/or physical vapour deposition (PVD) techniques. While there are numerous investigations of the electrochemistry of tin in aqueous solutions[9-12], it is less studied in ionic liquids or molten salts. Castrillejo *et al.*[13] studied the electrochemistry of Sn(II) with voltammetry, chronopotentiometry and chronoamperometry at glass carbon (GC) and W electrodes in the high-temperature molten salt system at 450 ºC. They observed that Sn(IV)/Sn(II) and Sn(II)/Sn redox couples were quasi-reversible. Hussey *et al.*[14] investigated the electrochemistry of Sn(IV) and Sn(II) with voltammetry and chronoamperometry at several different electrodes in the $AlCl_3$-EMIC ionic liquids at 40 ºC. They found that the Sn(II) reduction was uncomplicated at Pt and the underpotential deposition of Sn occurs at Au. Furthermore, the deposition of Sn at glass carbon was complicated by 3D nucleation. They also reported that voltammetric oxidation of Sn(II) to Sn(IV) was hindered by the weak adsorption of Sn(II). Tachikawa *et al.*[15] obtained a smooth dense faceted Sn deposits from a hydrophobic *N*-butyl-*N*-methylpyrrolidinium *bis*(trifluoromethylsufonyl)imide (BMP-NTf_2) room temperature ionic liquid, whereas Sun *et al.*[6] reported that the macroporous tin could be well electrodeposited in a water- and air-stable room temperature ionic liquid, namely, 1-ethyl-3-methylimidazolium-dicyanamide (EMI-DCA) room temperature ionic liquid. Recently, Martindale *et al.*[16] compared the microelectrode voltammetry of the Sn(II)/Sn couple in BMP-NTf_2 and BMP-DCA room temperature ionic liquids using solutions prepared by dissolution of $SnCl_2$ and $Sn(CF_3SO_3)_2$. They found that the diffusion coefficient Sn(II) species varied with the room temperature ionic liquids as well as the Sn(II) salts used, reflecting that different Sn(II) species were present. Furthermore, while a large difference in the voltammetry of the different Sn(II) salts was seen in BMP-NTf_2, the mechanism for the Sn stripping process is largely similar for Sn(II) salts

in BMP-DCA, implying that the morphology of the Sn deposit could be similar.

Although water- and/or air-stable room temperature ionic liquids are potentially useful for electrochemical studies[17], there is a paucity of imformation about the electrochemistry of metals in these room temperature ionic liquids. As a continuation of this research effort, the electrochemical behaviour of Sn(II)/Sn on platinum and glass carbon electrode in the non-Cl^- $[EMIm]BF_4$ ionic liquid at ambient temperature was investigated. The formal potential of the Sn(II)/Sn couple ($E^{0'}$), standard heterogeneous rate constant (k^0), transfer coefficient (α) and diffusion coefficient of Sn(II) (DSn(II)) were estimated. Furthermore, the electrodeposition behaviour of Sn(II) was studied in this work.

EXPERIMENTAL

The 1-ethyl-3-methylimidazolium tetrafluoroborate ionic liquid was a commercial product (Hangzhou Chemer Chemical Co. Ltd, 98 %) and was purified according to the method described in the literature[3]. The density, absolute viscosity (η) and conductivity of this ionic liquid at 25 ºC were determined to be 1.2416 g cm^{-3}, 0.357 g cm^{-1} s^{-1} and 1.37 × 10^{-2} S cm^{-1}, respectively. Tin(II) tetrafluoroborate ($Sn(BF_4)_2$, EHSY Lab) was used as received.

Detection method: All the electrochemical experiments were carried out under the air atmosphere. A CHI 660B electrochemical testing system (CH Instruments, Inc.) with a three-electrode electrochemical cell was employed to conduct the electrochemical experiments. For voltammetry and chronoamperometry, the working electrode was either a platinum disk (A = 1.96 × 10^{-3} cm^2, Aldrich 99.99 %) or a glass carbon electrode (A = 0.071 cm^2, Pine Instrument Co.). The counter electrode was a platinum wire (0.5 mm diameter, Aldrich 99.99 %) spiral immersed in pure ionic liquid contained in a glass tube having a fine porosity tip. The reference electrode was a spiral silver electrode immersed in the $[EMIm]BF_4$ liquid saturated with $AgBF_4$, which was separated from the bulk ionic liquid electrolyte through G4 glass filter. All the electrode potentials reported in this paper are relative to this reference electrode. Electrodeposition was conducted on a platinum wire (0.5 mm diameter, Aldrich 99.99 %). The electroplated wires were immersed in deoxidized acetone for a few minutes, washed with ethanol and deionized water in sequence to remove the ionic liquid residue. A field emission scanning electron microscope (SEM) (FEI QUANTA-200) with an energy dispersive X-ray spectroscopy (EDX) working at 30 kV was used to examine the surface morphology and analyze the element compositions of the electrodeposits.

RESULTS AND DISCUSSION

Electrodissolution of tin: The pure $[EMIm]BF_4$ ionic liquid exhibits an electrochemical window of 4.0 V ranging from *ca.* 2.4V to -1.6 V *vs.* Ag/Ag(I). Sn(II) was introduced into the $[EMIm]BF_4$ by the addition of high purity of $Sn(BF_4)_2$. The solubility of $Sn(BF_4)_2$ in $[EMIm]BF_4$ at room temperature was found to be approximately 0.13 mol dm^{-3} by visual observation.

A Nernst plot was constructed for the Sn(II)/Sn couple in the $[EMIm]BF_4$ ionic liquids by using controlled-potential electrolysis to vary the Sn(II) concentration in solutions contained in an electrochemical cell equipped with the Ag/Ag(I) reference electrode and a Sn indicator electrode. The potential, E, depended linearly on the logarithmic concentration of Sn(II), $C_{Sn(II)}$, in mol dm^{-3} with a slope of 29.8 mv/dec, as shown in Fig. 1. The dependence of the potential on the concentration of Sn(II) was represented by a Nernst equation as follows:

$$E = E^{0'} + \frac{2.303RT}{nF}\log C_{Sn(II)} \quad (1)$$

where, $E^{0'}$, R, T, n and F are formal potential in V, gas constant in J mol^{-1} K^{-1}, absolute temperature in K, number of electrons and Faraday constant in C mol^{-1}, respectively. The slope was in good agreement with the theoretical value (29.5 mv) for a two-electron process at 25 ºC. The intercept of the plot, which corresponds to the formal potential, $E^{0'}$, of Sn(II)/Sn couple was -0.60V.

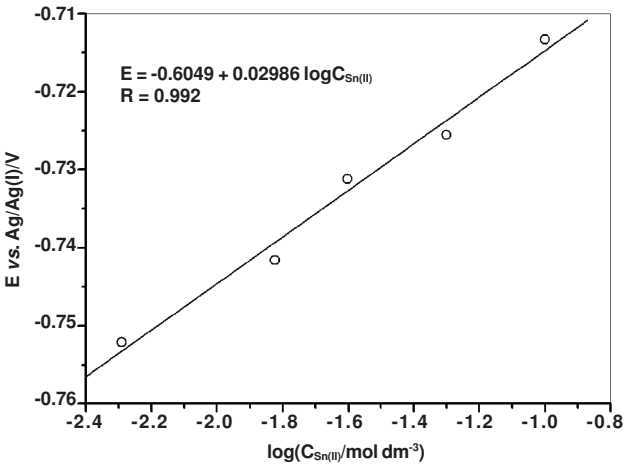

Fig. 1. Nernst plot of Sn(II)/Sn couple in the $[EMIm]BF_4$ ionic liquid at room temperature

Electrochemical behaviour of the Sn(II)/Sn couple: Typical cyclic voltammograms (CVs) recorded at both Pt and glass carbon electrodes of a 30 mmol dm^{-3} Sn(II) at 25 ºC were shown in Fig. 2. A Pair of cathodic and anodic current peaks was observed at *ca.* -0.7V. The potentiostatic cathodic reduction at -0.8V on a Pt electrode gave a white deposit without brightness. The EDX analysis of the electro-deposit showed the existence of Sn metal, indicating that the cathodic current wave, c_1, was due to the reduction of Sn(II) to Sn metal. Upon scan reversal at -0.9V, the stripping of the electrodeposited Sn metal occurs at wave a_1. The integrated charge from this stripping wave equals the charge corres-ponding to wave c_1 revealed that virtually 100 % of the deposited Sn is recovered during oxidation. In addition, a nucleation loop that was associated with electrodeposition processes requiring nucleation over potentials was seen on glass carbon electrode.

The effects of scan rate, ν, on the cyclic voltammograms of a Pt electrode in the $[EMIm]BF_4$ ionic liquids were shown in Fig. 3. Overall, the voltammetric waves for the deposition and stripping of Sn at Pt electrode with the different scan rate were unremarkable in appearance, *i.e.*, they do not exhibit obvious differences seen in Fig. 3. The typical cyclic voltammograms data of 25 mM Sn(II) in the $[EMIm]BF_4$ ionic liquid at various potential scan rates, ν(mV s^{-1}), are given in

TABLE-1
CYCLIC VOLTAMMOGRAMS DATA FOR THE 25 mM Sn(II) IN THE [EMIm]BF_4 IONIC LIQUID ON Pt ELECTRODE AT ROOM TEMPERATURE

ν (mV s^{-1})	$10^6 i_p^c$ (A)	$10^5 i_p^c/\nu^{1/2}$ /A $s^{1/2}$ $V^{-1/2}$	E_p^c (V)	E_p^a (V)	$E_{p/2}^c$ (V)	$/E_p^c - E_{p/2}^c/^a$ (V)	$/E_p^c - E_p^a/^b$ (V)
5	1.955	2.77	-0.6463	-0.5833	-0.7060	0.0203	0.0633
10	2.771	2.76	-0.6515	-0.5830	-0.7260	0.0210	0.0685
20	3.587	2.53	-0.6875	-0.5886	-0.7380	0.0334	0.0989
50	5.502	2.46	-0.6966	-0.5869	-0.7340	0.0367	0.1097
100	7.049	2.23	-0.7073	-0.5912	-0.7610	0.0393	0.1161

[a]Theoretical value for a reversible deposition reaction at 25 ºC is 0.0565/n V[18]; [b] Value for a reversible reaction at 25 ºC is 0.059/n V[23]

Table-1. However, the cathodic peak potential, E_p^c, shifted to the more negative side, the peak current function, $i_p^c/\nu^{1/2}$, decreased and the peak potential- half-peak potential separation, $/E_p^c - E_p/_2^c/$, increased as the scan rate was increased (Table-1). At the low scan rate examined, the parameter $/E_p^c - E_p/_2^c/$ approached the 0.0282V theoretical value expected for the two-electron reversible deposition reaction at 25 ºC[18]. The peak potential separation, $/E_p^c - E_p^a/$, exceeded 60 mV, while the value for a reversible reaction at 25 ºC is 29.5 mV and increased rapidly as the scan rate, ν, was increased. Since the current applied is in the range of a few microamperes, the effect of ohmic drop in the electrolyte should be negligible[19]. Taken together, these results suggest that the deposition of Sn at Pt electrode was a quasi- or irreversible process due to the slow electron transfer.

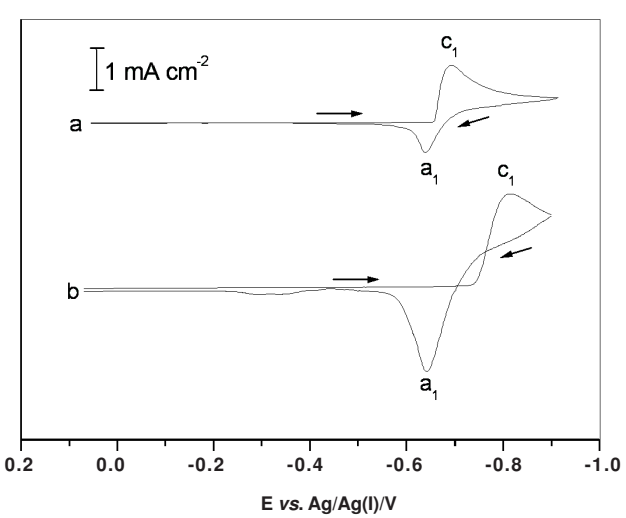

Fig. 2. Cyclic voltammograms of 25 mmol dm^{-3} Sn(II) in the [EMIm]BF_4 ionic liquids at 25 ºC, (a) Pt electrode; (b) glass carbon electrode. The scan rate was 50 mV s^{-1}

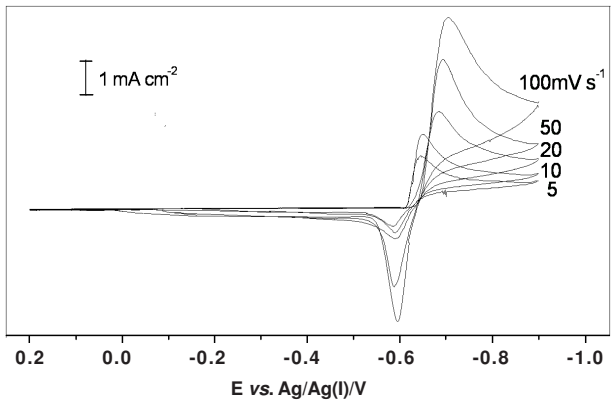

Fig. 3. Cyclic voltammograms of a Pt electrode in the [EMIm]BF_4 ionic liquid containing 25 mmol dm^{-3} Sn(II) at various scan rates

Determination of the kinetic parameters of the Sn(II)/Sn couple: The transfer kinetics of the Sn(II)/Sn couple at Pt electrode in the [EMIm]BF_4 ionic liquid was further studied. The standard heterogeneous rate constant, k^0 and the transfer coefficient, α, for reduction of Sn(II) to Sn was estimated from the cyclic voltammograms of the reduction Sn(II) by plotting the logarithm of the peak current density, j_p, *vs*. the difference of the peak potential and the formal potential, $E_p - E^{0'}$, as shown in Fig. 4, according to the following equation[20].

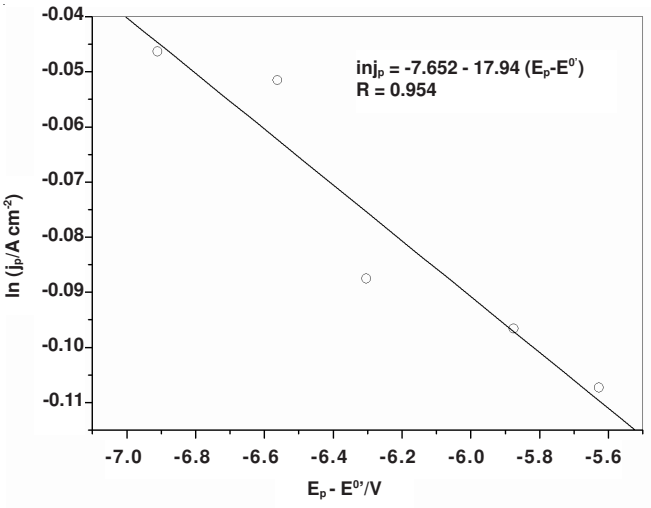

Fig. 4. Plots of ln j_p *vs*. $E_p - E^{0'}$ determined at different scan rate. The data were taken from the cyclic voltammograms for the reduction of 30 mM Sn(II) at Pt electrode in the [EMIm]BF_4 ionic liquid at 25 ºC

$$\ln j_p = \ln(0.227 n_a F C_{Sn(II)} k^0) - \alpha n_a F/RT(E_p - E^{0'}) \quad (2)$$

where n_a, R, T and F are the number of electrons involved in the electrochemical reduction, gas constant (J mol^{-1} K^{-1}), absolute temperature (K) and Faraday constant (C mol^{-1}), respectively. The values of a and k^0 were estimated from the slope and the intercept of Fig. 4, respectively. The diffusion coefficient of Sn(II) ($D_{Sn(II)}$) for reduction of Sn(II) to Sn was estimated by plotting the peak current density j_p *vs*. the square root of scan rate, ν, as shown in Fig. 5, from the following equation[20].

$$j_p = 2.99\times10^5 n(\alpha n_a)^{1/2} C^*_{Sn(II)} D^{1/2}_{Sn(II)} \nu^{1/2} \quad (3)$$

where $C^*_{Sn(II)}$ stands for the bulk concentration of Sn(II) in mmol dm^{-3}. The $D_{Sn(II)}$ value was estimated from the slope of Fig. 5. The results were collected in Table-2. As shown in this table, the k^0 value, 3.61×10^{-4} cm s^{-1}, was rather smaller than those reported in aqueous solution systems without complexing agents, $k^0 = 1 \times 10^{-2}$ cm s^{-1} in KNO_3 solution, for example[21]. The quasi- or irreversible behaviour of the reduction of Sn(II) had also been investigated in $ZnCl_2$-[EMIm]BF_4[15] and in $AlCl_3$-

TABLE-2
KINETIC PARAMETERS OF THE ELECTROCHEMICAL REDUCTION OF 30mM Sn (II) IN THE $[EMIm]BF_4$ IONIC LIQUID ON Pt ELECTRODE AT 25 ºC

System	Electrode	α	k^0 (cm s^{-1})	$10^7 D_{Sn(II)}$ (cm^2 s^{-1})	$10^{10}\eta D_{Sn(II)} T^{-1}$ (g cm s^{-2} K^{-1})
Non-Cl^- $[EMIm]BF_4$ (this work)	Pt	0.23	3.61×10^{-4}	9.85	11.8
Free-Cl^- $[EMIm]BF_4$[22]	Pt	0.537		6.07	7.27
$ZnCl_2$-$[EMIm]BF_4$[15]	W	0.36	2.50×10^{-7}	4.61	
$ZnCl_2$-$[EMIm]BF_4$[15]	GC	0.30	3.39×10^{-6}		
1.5:1 Acidic $AlCl_3$-[EMIm]Cl[14]	Pt			4.60	0.99
0.75:1 Basic $AlCl_3$-[EMIm]Cl[14]	Pt			5.32	3.55

[EMIm]Cl[14] system. The slow kinetics of the reduction of Sn(II) in these systems may be explained by the existence of the bulky $[EMIm]^+$ cation, which may cover the surface of the cathodically polarized electrode and obstruct the charge transfer[19]. However, this table indicates a larger k^0 was obtained at Pt electrode than at the W or glass carbon electrode, indicating that Sn(II)/Sn reduction at the Pt electrode is kinetically more favourable than at the W or glass carbon electrode.

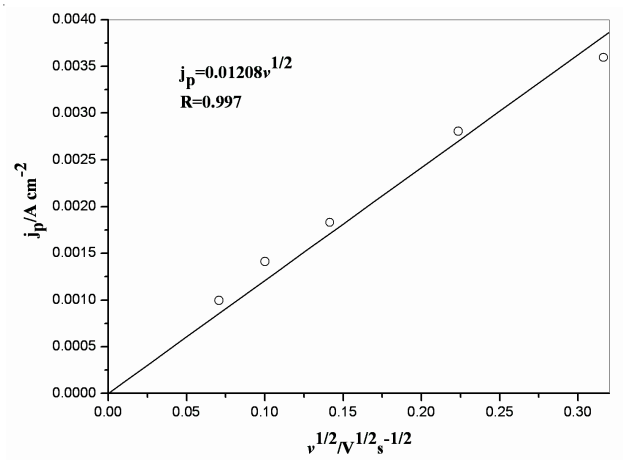

Fig. 5. Plots of j_p *vs.* $v^{1/2}$ determined at different scan rate. The data were taken from the cyclic voltammograms data for the reduction of 30 mM Sn(II) at Pt electrode in the $[EMIm]BF_4$ ionic liquid at 25 ºC

The diffusion coefficient is related to the viscosity of the solution, η and the solvodynamic radius of a diffusing species, r_{solv}, according to the Stokes-Einstein equation.

$$D = \frac{kT}{6\pi\eta r_{solv}} \quad (4)$$

where, k is the Boltzman constant. The Stokes-Einstein product, $\eta D_{Sn(II)}/T$, is inversely proportional to the solvodynamic radius. The $\eta D_{Sn(II)}/T$ value of Sn(II) in the non-Cl^- $[EMIm]BF_4$ system is 11.8×10^{-10} g cm s^{-2} K^{-1}, which is larger than that of Sn(II) in free-Cl^- $[EMIm]BF_4$ system 22, 7.27×10^{-10} g cm s^{-2} K^{-1} and in acidic, 0.99×10^{-10} g cm s^{-2} K^{-1}, or basic, 3.55×10^{-10} g cm s^{-2} K^{-1}, $AlCl_3$-[EMIm]Cl ionic liquid[14]. Comparing this result with previous one, the smaller $\eta D_{Sn(II)}/T$ value of Sn(II) may be attributed to the simpler Sn(II) chloro complex species in the free-Cl^- $[EMIm]BF_4$ than that in the $AlCl_3$-[EMIm]Cl[22]. On the other hand, the larger $\eta D_{Sn(II)}/T$ value of Sn(II) in non-Cl^- $[EMIm]BF_4$ than in free-Cl^- $[EMIm]BF_4$, suggesting that Sn(II) may exist in the form of a simple cation in non-Cl^- $[EMIm]BF_4$.

Nucleation studies of Sn electrodeposition in $[EMIm]BF_4$: The cyclic voltammograms in Fig. 2b exhibit a current loop that is typical of a deposition process requiring nucleation overpotential. The nucleation process at glass carbon electrode was further investigated by chronoamperometry in unstirred $[EMIm]BF_4$ ionic liquid containing 30 mM Sn(II) by stepping the potential from -0.6V, where no reduction of Sn(II) would occur, to potentials sufficient negative to initiate the nucleation/growth process after a short induction time, t_0. Typical current-time transients resulting from such experiments are shown in Fig. 6. At low overpotential, the transients exhibit the classic sharp for a nucleation process with diffusion-controlled growth, *i.e.*, after a double-layer capacitive current decay, the faradaic current increases slowly then decreases after reaching a current maximum, i_M. The time to reach this current maximum is t_M, which decreases as the applied overpotential is increased. The three-dimensional (3D) nucleation/growth process is fundamentally described as either "instantaneous" or "progressive"[12]. Instantaneous model refers to the situation in which all nucleation sites is activated at the beginning of the chronoamperometric experiments, whereas progressive model refers to the situation in which the nucleation sites gradually become activated as the chronoampero-metric experiment proceeds. The type of nucleation often affects the morphology of the electrodeposits.

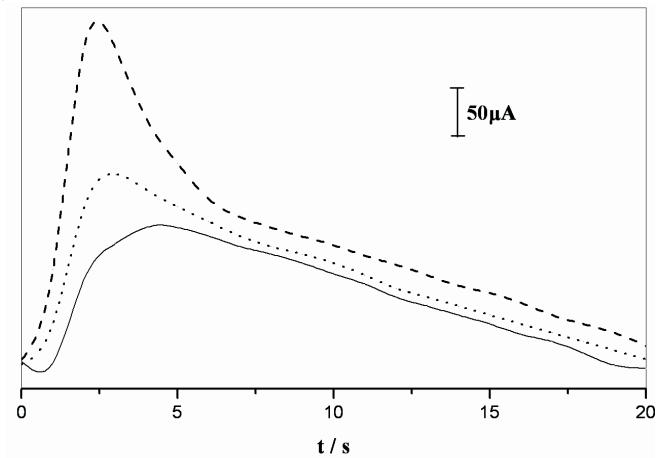

Fig. 6. Current-time transients resulting from chronoamperometric experiments of 30 mM Sn(II) on glass carbon electrode in $[EMIm]BF_4$ ionic liquid at 25 ºC: (.....) -0.80 V, (**.....**) -0.85 V, (.....) -0.90 V

One of methods to determine the applicability of nucleation model is to compare current-time transients derived from potential-step experiments to the dimensionless theoretical curves for instantaneous and progressive nucleation which were described by equation (5) and (6), respectively.

$$(i/i_M)^2 = 1.9542/(t/t_M)\{1 - \exp[-1.2564(t/t_M)]\}^2 \quad (5)$$

$$(i/i_M)^2 = 1.2254/(t/t_M)\{1-\exp[-2.3367(t/t_M)^2]\}^2 \quad (6)$$

Before the analysis, the experimental time was corrected for the induction time by redefining the time axis as $t' = t-t_0$ and $t_M' = t_M - t_0$. Estimates of t_0 were obtained from the intercepts of the plots of $(i/i_M)^2$ or $(i/i_M)^{2/3}$ *vs*. t, in these cases, t_0 is less than 1.0 s. The representative experimental plot for Sn electrodeposition overlaid with the theoretical curves is shown in Fig. 7. This figure clearly shows that the deposition of Sn on glass carbon electrode fits well to the model for 3D instantaneous nucleation. Similar behaviour has been reported for the electrodeposition of Sn on glass carbon electrode in $ZnCl_2$-[EMIm]BF_4[15] and $AlCl_3$-[EMIm]Cl[14] systems.

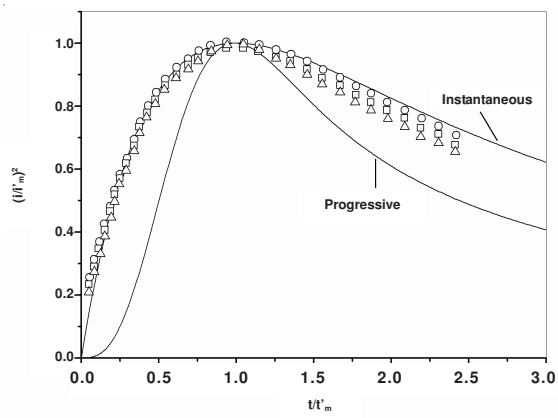

Fig. 7. Comparison of dimensionless experimental current-time transients derived from chronoamperometric experiments for 30 mM Sn(II) in [EMIm]BF_4 ionic liquid at 25 ºC on glass carbon electrode with theoretical models for three-dimensional nucleation process: (O) -0.80 V, (□) -0.85 V, (△) -0.90 V

Bulk electrodeposition of tin: The electrodeposition experiments were carried out in the [EMIm]BF_4 ionic liquid containing 30 mM Sn(II) at room temperature. The metal deposits were plated on 0.5 mm diameter platinum wires under the atmosphere of argon. The potential of electrodeposition was controlled at -1.1 V *vs*. Ag/Ag(I). The metal plated wires were then immersed in pure acetone solvent for a few minutes, rinsed with ethanol and deionized water in sequence to remove the melt residue.

The surface morphology and EDX analysis of the deposits are presented in Fig. 8. It revealed that they were pure metals without other elemental contaminants, such as Cl, B and F, indicating that no ionic liquid residue was left on the deposit surfaces. As shown in Fig. 8, the Sn deposit produced at -1.1 V *vs.* Ag/Ag(I) was just needle-type islands, not a continuous plating film on Pt surface.

Conclusion

The electrochemistry of Sn(II) was studied in terms of cyclic voltammetry and chronoamperometry. The reduction of Sn(II) on Pt electrode exhibits the electrochemically irreversible behaviour. The diffusion coefficient and Stoke-Einstein products calculated from cyclic voltammograms data for Sn(II) indicated that Sn(II) may exist as bare cation in non-Cl-[EMIm]BF_4 without complexing agents. The electrodeposition of Sn(II) at glass carbon electrode was complicated by nucleation. Experimental current-time transients are in good agreement with the theoretical model based on 3D nucleation. The morphology examined by SEM of the electrodeposit indicates that the Sn deposit is not a continuous plating film on Pt surface.

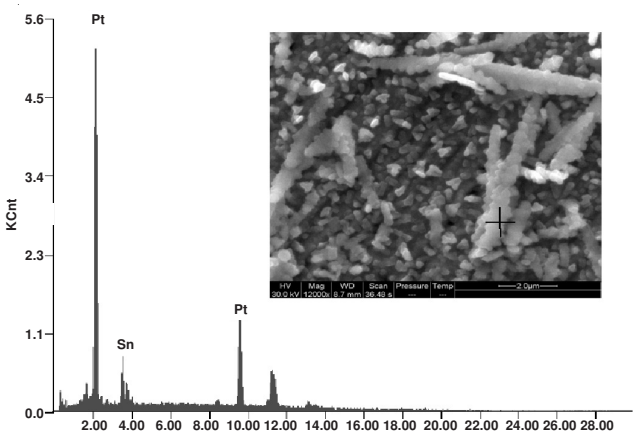

Fig. 8. SEM micrograph and EDS spectra of Sn deposits that were prepared from the [EMIm]BF_4 ionic liquid containing 30 mM Sn(II) at room temperature. Electrodeposition potential was -1.1V *vs*. Ag/Ag(I)

ACKNOWLEDGEMENTS

This work was funded by the Applied Basic Research Project of Yancheng Institute of Technology of Chian, Jiangsu (Grant no. XKR2011005).

REFERENCES

1. T. Welton, *Chem. Rev.*, **99**, 2071 (1999).
2. M.J. Earle and K.R. Seddon, *Pure Appl. Chem.*, **72**, 1391 (2000).
3. Y.H. Pang, X.Y. Li, G.Y. Shi, F. Wang and L.T. Jin, *Thin Solid Films*, **516**, 6512 (2008).
4. R. Al-Salman, X.D. Meng, J.P. Zhao, Y. Li, U. Kynast, M.M. Lezhnina and F. Endres, *Pure Appl. Chem.*, **82**, 1673 (2010).
5. R.T. Kachoosangi, M.M. Musameh, I.A. Yousef, S.M. Kanan, L. Xiao, S.G. Davies, A. Russell and R.G. Compton, *Anal. Chem.,* **81**, 435 (2009).
6. M.J. Deng, T.I. Leong, I.W. Sun, P.-Y. Chen, J.-K. Chang and W.-T. Tsai, *Electrochem. Solid State Lett.*, **11**, D85 (2008).
7. S.Z.E. Abedin, P. Giridhar, P. Schwab and F. Endres, *Electrochem. Commun.*, **12**, 1084 (2010).
8. A.P. Abbott, Ttaib K. El, K.S. Ryder and E.L. Smith, *Trans. Inst. Met. Finish.*, **86**, 234 (2008).
9. A. Brenner, Electrodeposition of Alloys, Principles and Practice. Academic Press, New York, (1963).
10. R. Einand, M. Schlesinger and M. Paunovic, In Modern Electroplating, John Wiley & Sons, New York (2000).
11. S. Vitkova, V. Ivanova and G. Raichevsky, *Surf. Coat. Technol.*, **82**, 226 (1996).
12. C.T.J. Low and F.C. Walsh, *Electrochim. Acta*, **53**, 5280 (2008).
13. Y. Castrillejo, M.A. Garcia, A.M. Martinez, C. Abejon, P. Pasquier and G. Picard, *J. Electroanal. Chem.*, **434**, 43 (1997).
14. X.H. Xu and C.L. Hussey, *J. Electrochem. Soc*., **140**, 618 (1993).
15. N. Tachikawa, N. Serizawa, Y. Katayama and T. Miura, *Electrochim. Acta,* **53**, 5280 (2008).
16. B.C.M. Martindale, S.E.W. Jones and R.G. Compton, *Phys. Chem. Chem. Phys.*, **12**, 1827 (2010).
17. F.A. Cotton and G. Wilkinson, Advanced Inorganic Chemistry, Wiley, New York (1988).
18. G. Mamantov, D.L. Manning and J.M. Dale, *J. Electroanal. Chem.*, **9**, 253 (1965).
19. T. Tomiyama, R. Toita, J.-H. Kang, D. Asai, S. Shiosaki, T. Mori, T. Niidome and Y. Katayama, *J. Electrochem. Soc*., **148**, 102 (2001).
20. A.J. Bard, L.R. Faulkner, Electrochemical Methods: Fundamentals and Applications, John Wiley & Sons, New York (1980).
21. R. Parsons, Handbook of Electrochemical Data, Butterworths, London (1959).
22. W.Z. Yang, H. Cang, Y.M. Tang, J.T. Wang and Y.X. Shi, *J. Appl. Electrochem.*, **38**, 537 (2008).